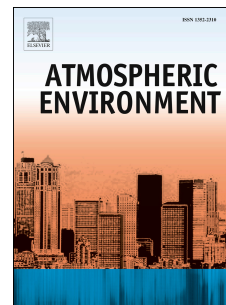


# Accepted Manuscript

Analysis for Sources of Atmospheric  $\alpha$ - and  $\gamma$ -HCH in Gas and Particle-associated Phase in Dalian, China by Multiple Regression

Qingbo Li, Yan Li, Xianyu Wang, Ruiqi Zhang, Jianmin Ma, Mengxue Sun, Xiaoning Lv, Jiaoling Bao



PII: S1352-2310(15)30098-4

DOI: [10.1016/j.atmosenv.2015.05.025](https://doi.org/10.1016/j.atmosenv.2015.05.025)

Reference: AEA 13832

To appear in: *Atmospheric Environment*

Received Date: 30 June 2014

Revised Date: 11 May 2015

Accepted Date: 13 May 2015

Please cite this article as: Li, Q., Li, Y., Wang, X., Zhang, R., Ma, J., Sun, M., Lv, X., Bao, J., Analysis for Sources of Atmospheric  $\alpha$ - and  $\gamma$ -HCH in Gas and Particle-associated Phase in Dalian, China by Multiple Regression, *Atmospheric Environment* (2015), doi: 10.1016/j.atmosenv.2015.05.025.

This is a PDF file of an unedited manuscript that has been accepted for publication. As a service to our customers we are providing this early version of the manuscript. The manuscript will undergo copyediting, typesetting, and review of the resulting proof before it is published in its final form. Please note that during the production process errors may be discovered which could affect the content, and all legal disclaimers that apply to the journal pertain.

1 **RUNNING HEAD:** Analysis for Sources of Atmospheric  $\alpha$ - and  $\gamma$ -HCH in Gas and Particle-associated Phase in  
2 Dalian, China by Multiple Regression

3  
4

5 **Corresponding Author:** Qingbo Li

6 **ADDRESS:** College of Environmental Science and Engineering, Dalian Maritime University,  
7 Dalian 116026, China

8 **PHONE:** 86-0411-84727771

9 **FAX:** 86-0411-84727771

10 **E-MAIL:** drliqb@gmail.com

11

12 Analysis for Sources of Atmospheric  $\alpha$ - and  $\gamma$ -HCH in Gas and Particle-associated Phase in Dalian, China by  
13 Multiple Regression

14 QINGBO LI\*<sup>†</sup>, YAN LI<sup>††</sup>, XIANYU WANG<sup>††</sup>, RUIQI ZHANG<sup>†††</sup>, JIANMIN MA<sup>††††</sup>, MENGXUE SUN<sup>†</sup>,  
15 XIAONING LV<sup>†</sup>, JIAOLING BAO<sup>†</sup>

16 <sup>†</sup> College of Environmental Science and Engineering, Dalian Maritime University, Dalian 116026, China

17 <sup>††</sup>National Research Centre for Environmental Toxicology, The University of Queensland, 39 Kessels Road,  
18 Coopers Plains, QLD, 4108, Australia

19 <sup>†††</sup>Shaanxi University of Science & Technology, Shaanxi 710021, China

20 <sup>††††</sup>Key Laboratory of Western China's Environmental System, Ministry of Education, College of Earth and  
21 Environment Sciences, Lanzhou University, Lanzhou 730000, China

22  
23  
24  
25  
26  
27  
28  
29  
30  
31  
32  
33  
34  
35  
36  
37  
38  
39  
40  
41  
42  
43  
44  
45  
46  
47  
48

\*Corresponding author phone: +86 411 8472-7771; fax: +86 411 8472-7771; e-mail: drliqb@gmail.com

49 **Abstract:**

50

51 Atmospheric concentrations of  $\alpha$ - and  $\gamma$ -hexachlorocyclohexanes were measured once a week in Dalian throughout  
52 2008, using a high-volume air sampler, to estimate diurnal, monthly and seasonal variations. Multiple regression  
53 analysis was used to estimate the impact of selected meteorological conditions on atmospheric concentrations of  
54 hexachlorocyclohexanes and to identify the potential source regions. Overall,  $\alpha$ - and  $\gamma$ -hexachlorocyclohexanes were  
55 mainly associated with the gas phase, with an annual mean gas-phase concentration of  $36\pm 30$  and  $10\pm 9.8$   $\text{pg m}^{-3}$   
56 respectively. On the other hand, mean particle ( $\text{PM}_{10}$ ) associated concentrations throughout the year were  $1.9\pm 2.4$   
57 and  $0.46\pm 0.43$   $\text{pg m}^{-3}$  respectively. Gas-phase concentration of  $\alpha$ - and  $\gamma$ -hexachlorocyclohexanes peaked in the  
58 autumn season whereas highest concentrations in the particle phase were measured in spring. Ratio of  $\alpha$ -/ $\gamma$ -isomer  
59 ranged from 3.7 to 7.4 in the gas phase which was close to the ratio in technical hexachlorocyclohexanes (5~7). In  
60 the particle-associated phase this ratio ranged from 1.2 to 3.8, with the exception of daytime samples in spring (up to  
61 16) and summer seasons (up to 14) and this exception could be due to the isomerization from  $\gamma$ - to  $\alpha$ - in ambient air,  
62 at least partly resulted from the impact of sunlight. Regression analysis showed that, at the sampling site,  
63 concentrations of  $\alpha$ - and  $\gamma$ -hexachlorocyclohexanes in the gas phase were both elevated with increasing temperature  
64 and wind speed, whereas in the particle-associated phase their concentrations tended to remain stable.

65

66

67 **Keywords:** Hexachlorocyclohexanes; Gas phase; Particle-associated phase; Multiple Regression; Sources

68

69

70

71

72

73

74

75

76

77

78

79

80

81

82

83

## 84 **1. Introduction**

85  
86 Hexachlorocyclohexanes (HCHs) were used extensively between the 1960s and the 1980s and cumulative  
87 consumption of technical HCHs has been estimated as 6 million tons globally (Willett, Ulrich, & Hites, 1998). In  
88 China, HCHs were widely used for agricultural purposes and vector control and the amount of technical HCHs used  
89 in China and South Asia during the late 1970s was estimated at about 60,000 tons per year (Willett et al., 1998).  
90 During and after application, large amounts of HCHs can be released and condensed into environmental reservoirs  
91 such as soil, vegetation and cryosphere. Subsequently, the stored HCHs can re-volatilize from these secondary  
92 sources into environmental compartments and can result in exposure of humans and the whole ecosystem.  
93 Temperature is invoked as the major controller for semi-volatile organic compounds (SVOCs) such as HCHs to  
94 condense into/(re-)volatilize from environmental reservoirs, effectively accounting for their cycling nature between  
95 air and earth's surfaces (Halsall et al., 1999). Several studies have interpreted this phenomenon using the  
96 Clausius-Clapeyron equation, in which chemical concentrations in air, expressed as partial pressure, are plotted  
97 against ambient temperature (Hoff, Mulr, & Grift, 1992; Hornbuckle & Eisenreich, 1996; Venier & Hites, 2010).  
98 Besides, wind speed and direction are also considered as the major factors, which can be integrated into a multiple  
99 regression model including also reciprocal temperature, to interpret the impact of these meteorological parameters  
100 on the concentrations of SVOCs in ambient air. For example, Hillery et al. used this equation to relate atmospheric  
101 PCB concentrations to meteorological conditions, thereby to study the temporal and spatial trends of gas-phase PCB  
102 concentrations near the Great Lakes (Hillery, Basu, Sweet, & Hites, 1997).

103  
104 Dalian is a seaside city where the distribution of atmospheric pollutants could be influenced by diel cycle of sea-land  
105 breeze. However, to our best knowledge, limited reports are available for diurnal and seasonal variations of  
106 organochlorine pesticides (OCPs) including HCHs (Li et al., 2012; Li et al., 2011) and for their source analysis  
107 within this city. This study aims to obtain diurnal and seasonal data for atmospheric HCHs in Dalian air and to  
108 analysis their sources by a multiple regression model both in the gas and particle-associated phase.

109

## 110 **2. Materials and methods**

111

### 112 **2.1 Sample collection**

113 The sampling site is located in Dalian (121°31'E, 38°52'N), in the southern tip of Liaodong peninsular in northeast  
114 China, adjacent to the Yellow Sea and Bohai Sea (the supplementary information (SI) Figure S1). The city locates in  
115 the temperate zone featured by a typical maritime continental monsoon climate. A sampling platform (altitude 12 m

116 above the ground) is mounted on the Technology Building of Dalian Maritime University and is ~10 km to the city  
117 center and ~1 km to the Yellow Sea and lacks of major proximate OCP sources. Detailed sampling method has been  
118 published elsewhere (Li et al., 2012). Briefly, a high-volume air sampler operating at a flow rate at about 1.0 m<sup>3</sup>  
119 min<sup>-1</sup> was used to collect gas-phase and particle (PM<sub>10</sub>)-associated-phase samples simultaneously once a week  
120 throughout the year of 2008. This sampling platform is also equipped with a mini weather station (Watchdog  
121 900ET) for monitoring and recording meteorological parameters continuously, including wind speed and direction,  
122 ambient temperature, relative humidity and solar radiance at the height analogues to that the air sampler was  
123 mounted. Data were recorded automatically every 6 seconds into a data-logger and output as hourly mean values.

124

## 125 **2.2 Sample analysis**

126 Sample extraction, cleanup and analysis were published in detail elsewhere (Li et al., 2012). Briefly, samples were  
127 extracted by *n*-hexane and cleaned up by a silica gel/neutral alumina column. Sample analysis was performed with a  
128 Shimadzu 2010 gas chromatograph (GC) equipped with a micro electron capture detector (*m*-ECD).

129

## 130 **2.3 Quality control and quality assurance (QC/QA)**

131 Detailed QC/QA procedure was reported elsewhere (Li et al., 2012). In brief, limits of detection (LOD) for  $\alpha$ - and  
132  $\gamma$ -HCH in the gas phase are 0.071 and 0.37 pg m<sup>-3</sup> respectively and in the particle phase, LOD for  $\alpha$ - and  $\gamma$ -HCH  
133 were 0.033 and 0.052 pg m<sup>-3</sup>, respectively.

134

## 135 **2.4 Multiple regressions**

136 Measured concentrations (pg m<sup>-3</sup>) of  $\alpha$ - and  $\gamma$ -HCH were converted to partial pressures (atm) using the ideal gas law.  
137 Air temperature (*T* in K) and wind speed (WS in mph) were regressed into the logarithms of the atmospheric partial  
138 pressures (Hillery et al., 1997):

139

$$140 \ln P = b_0 + b_1 (1/T) + b_2 WS + b_3 \sin WD + b_4 \cos WD, \quad (1)$$

141

142 where *b*<sub>0</sub> is an intercept and *b*<sub>1</sub> and *b*<sub>2</sub> describes the dependence of the partial pressure on reciprocal *T* and WS  
143 respectively; *b*<sub>3</sub> and *b*<sub>4</sub> are coefficients of the sine WD (wind direction in degree) and the cosine WD terms.

144 Two different methods, enter and stepwise method, which are fitted using IBM SPSS statistics 19, are used to run  
145 the multiple regression model separately.

146

## 147 **3. Results and discussion**

### 148 **3.1 Ambient concentrations of HCHs in Dalian atmosphere**

149  $\alpha$ -HCH. As expected,  $\alpha$ -HCH distributed mainly in the gas phase (ratio of  $C_{\text{gas}}/C_{\text{particle}}$  shown in SI Table S3), where  
150 a mean concentration of  $34\pm 27$  and  $32\pm 29$   $\text{pg m}^{-3}$  was measured during daytime and nighttime respectively  
151 throughout the year (SI Table S1). In contrast, in the particle-associated phase, one order of magnitude lower  
152 concentration was observed as  $1.6\pm 1.8$  and  $1.6\pm 2.1$   $\text{pg m}^{-3}$  during daytime and the nighttime, respectively (SI Table  
153 S2). As seen in Figure 1, in the gas phase, in terms of median concentration value in each month, the highest during  
154 daytime and nighttime was both observed in September at  $72$   $\text{pg m}^{-3}$  respectively. Whereas for particle-associated  
155  $\alpha$ -HCH, this value during daytime and nighttime was both measured in April, at  $2.8$  and  $3.5$   $\text{pg m}^{-3}$  respectively  
156 (Figure 2). Seasonally, concentration of gaseous and particle-associated  $\alpha$ -HCH peaked in autumn and spring season  
157 respectively both for daytime and nighttime (SI Table S1&S2).

158  
159  $\gamma$ -HCH. Similarly, dominant annual mean concentration was measured in the gas phase (SI Table S3), at  $10\pm 10$  and  
160  $11\pm 9.6$   $\text{pg m}^{-3}$  during the daytime and the nighttime respectively, compared to the one in the particle-associated  
161 phase at  $0.46\pm 0.38$  (daytime) and  $0.58\pm 0.56$   $\text{pg m}^{-3}$  (nighttime) (SI Table S1&S2). As shown in Figure 1, median  
162 value of  $\gamma$ -HCH concentration in the gas phase was highest in October (daytime, at  $18$   $\text{pg m}^{-3}$ ) and September  
163 (nighttime, also at  $18$   $\text{pg m}^{-3}$ ), respectively. In the particle-associated phase, on the other hand, this value was  
164 observed highest in January for the daytime (at  $0.59$   $\text{pg m}^{-3}$ ) and March for the nighttime (at  $1.0$   $\text{pg m}^{-3}$ ) (Figure 2).  
165 Seasonal variation of concentration of  $\gamma$ -HCH was similar to that of  $\alpha$ -HCH, as presented in SI Table S1&S2.

166  
167 **3.2 Isomer ratio ( $C_{\alpha\text{-HCH}}/C_{\gamma\text{-HCH}}$ ) and its indications**

168 The ratio of  $C_{\alpha\text{-HCH}}/C_{\gamma\text{-HCH}}$  is typically used as an indicator to trace origin and pathway of HCHs in the air (Iwata,  
169 Tanabe, Sakai, & Tatsukawa, 1993). As seen in SI Table S1&S2, this ratio for gaseous HCHs in each season ranged  
170 from 3.7 to 7.4, which was close to the ratio in technical HCHs (5~7), whereas in the particle-associated phase, this  
171 ratio was measured as 1.2 to 3.8, with the exception of daytime samples in spring (at 16) and summer seasons (at  
172 14). A possible reason for this higher ratio could be the significant isomerization of  $\gamma$ -isomer into  $\alpha$ -isomer, which  
173 has been experimentally demonstrated in the presence of ferrous salts and sunlight (Malaiyandi & Shah, 1984). That  
174 is, during the daytime,  $\gamma$ -isomer sorbed on the surface of particles may be isomerized intensively into the  $\alpha$ -isomer,  
175 resulted at least partly from the impact of sunlight.

176  
177 **3.3 Impact of meteorological conditions on atmospheric concentrations of HCHs**

178  
179 *Gas phase.* Under the enter method, as shown in Table 1, during daytime, integrated impact of temperature, wind  
180 velocity and wind direction on atmospheric concentrations of  $\alpha$ - and  $\gamma$ -HCH was found at significant level ( $R^2=0.41$

181 and 0.45 for  $\alpha$ - and  $\gamma$ -HCH respectively,  $p < 0.05$ ), whereas during nighttime it was only the case for  $\gamma$ -HCH  
182 ( $R^2 = 0.24$ ,  $p < 0.05$ ). Atmospheric concentration of  $\alpha$ - and  $\gamma$ -HCH at the sampling site both elevated with increased  
183 temperature and wind speed ( $b_1 < 0$  and  $b_2 > 0$ ). The correlation between concentration and temperature was  
184 statistically significant at  $p < 0.05$  during daytime for  $\alpha$ -HCH and both during daytime and nighttime for  $\gamma$ -HCH. For  
185 the correlation between concentration and wind speed, statistical significance ( $p < 0.05$ ) was observed only for  
186  $\alpha$ -HCH during daytime. The insignificant impact from wind direction for both isomers indicated that spatial  
187 variations of potential sources for atmospheric HCHs at the sampling site were probably not significant, i.e.  
188 re-emission from terrestrial and ocean surface does not cause significant variations of concentrations of HCHs in  
189 ambient air at the sampling site.

190  
191 As seen in Table 1, for both  $\alpha$ - and  $\gamma$ -HCH, the impact from temperature on concentrations was more significant (  $|$   
192  $b_1| \gg |b_2|$  ) compared to wind speed (although for  $\alpha$ -HCH neither reached a significant level at 0.05 during  
193 nighttime). Both of  $b_3$  and  $b_4$  were lower than 0 (and were marginally insignificant) for  $\alpha$ -HCH, indicating that  
194 atmospheric concentration at the sampling site may be influenced by  $\alpha$ -HCH transported by southwesterly wind. The  
195 area southwest of the sampling site is the Shandong Peninsular, which is the top province in China in terms of  
196 agricultural activities. Therefore, it is possible that gaseous  $\alpha$ -HCH in the atmosphere at the sampling site was  
197 (partly) from re-volatilization from the Shandong Peninsular and surrounding sea water reservoirs (presumably the  
198 historic residues) (the geographic information can be referred in the SI Figure S1). The results of the back trajectory  
199 analysis of the air masses during this sampling period also supported this interpretation (Li et al., 2012; Li et al.,  
200 2011). For both of  $\alpha$ - and  $\gamma$ -HCH,  $|b_1|$  was higher during daytime as compared with nighttime, indicating that  
201 the emission from terrestrial surfaces/reservoirs during the daytime exerted stronger impacts on their atmospheric  
202 concentrations, i.e. the influence of proximate sources was stronger on the concentrations at daytime than that on  
203 nighttime. Besides,  $|b_1|$  for  $\gamma$ -HCH was greater than that for  $\alpha$ -HCH during both of the daytime and nighttime,  
204 indicating that the influence of proximate sources was stronger on the atmospheric concentrations of  $\gamma$ -HCH  
205 compared to that of  $\alpha$ -HCH. Multicollinearity diagnostics of independent variables within equation (1) under the  
206 enter method were also carried out by evaluating eigenvalue, condition index, variance proportions and variance  
207 inflation factor (VIF). As shown in the SI Table S4, eigenvalue of dimension 5 was  $\leq 0.001$  and condition index was  
208 over 70 for each group and a high (1.0) variance proportion was detected for inverse  $T$  against dimension 5,  
209 indicating a possibility of multicollinearity inherent in the regression model between  $\cos WD$  and inverse  $T$ , although  
210 this was not supported by the low VIF ( $\approx 1$ ) (Jeeshim, 2003).

211



212 Given the insignificances and possible multicollinearity issue observed above for the enter method, a stepwise  
213 method was then applied for modelling gaseous HCHs and the result showed that the variable temperature can be  
214 included for  $\alpha$ - and  $\gamma$ -HCH during daytime and  $\gamma$ -HCH during night ( $P<0.002$ ) and sinWD can be included for  
215  $\alpha$ -HCH during night ( $P=0.026$ ) (SI Table S6), i.e. variations of concentrations of  $\alpha$ - and  $\gamma$ -HCH during daytime and  
216  $\gamma$ -HCH during night were mainly controlled by temperature (invoking re-volatilization from terrestrial and ocean  
217 surface). For  $\alpha$ -HCH at night time, although the above result indicated that the concentration could be controlled by  
218 contaminants delivered by wind from north, B value of variable sinWD was nevertheless two orders of magnitudes  
219 lower than the one of constant, which implied that the impact from north wind was limited.

220  
221 *Particle-associated phase.* As seen in Table 2, under the enter method, integrated impact of temperature, wind speed  
222 and wind direction on atmospheric concentrations of  $\alpha$ - and  $\gamma$ -HCH was found at insignificant level ( $p>0.05$ ), which  
223 implied that this model may be inadequate to explain/predict the variations of concentrations of particle-associated  
224 HCHs. Similarly to gaseous HCHs, possible multicollinearity was also observed for particle-associated HCHs under  
225 the enter method (SI Table S5). Thus the stepwise method was applied and modelling result showed that none of the  
226 parameters can be included, i.e. these parameters (temperature, wind speed and direction) exerted limited impact on  
227 the variation of concentrations of particle-associated HCHs. As seen in Figure 2, concentrations of  
228 particle-associated HCHs during daytime and night time were close to each other and no obvious monthly  
229 variations/differences can be observed (ANOVA  $P$  lies between 0.26 and 0.59). In addition, partial regression of  
230 concentrations of particle-associated HCHs (shown as  $\ln P$ ) against meteorological parameters, as seen in Figure  
231 3&4, showed scattered relationship, indicating their concentrations tended to remain stable rather than varying with  
232 these parameters. This result was opposite to that of another pesticide, endosulfan, analyzed from the same sample  
233 set, where an obvious monthly trend was observed, which was partly attributed to the changes of temperature and air  
234 mass origins between months (Li et al., 2012).

#### 235 236 **4. Conclusions**

237  
238 HCHs distribute mainly in the gas phase in Dalian air and mean concentration of  $\alpha$ -HCH is generally higher than  
239 that of  $\gamma$ -HCH. Concentration of gaseous and particle-associated HCHs peaks in autumn and spring respectively.  
240 The main controlling factor for gaseous HCH concentrations is ambient temperature and concentration of  
241 particle-associated HCHs tends to remain stable, i.e. temperature, wind speed and direction exert limited impact.  
242 Spatial variations of potential sources for atmospheric HCHs at the sampling site are probably not significant, i.e.  
243 re-emission from terrestrial and ocean surface does not cause significant variations of concentrations of HCHs in

244 ambient air at the sampling site. Emission characteristics from terrestrial and ocean surface should be further studied  
245 to illustrate spatial variations of potential sources for atmospheric HCHs.

246

247

248 *Acknowledgement* — This study was supported by the project of Natural Science Foundation of China (40671166,  
249 41371478 and 41371448). We acknowledge Dalian Meteorological Bureau for providing meteorological  
250 information for this study. We appreciate the anonymous reviewers for their valuable comments on an earlier  
251 version of the manuscript.

252

253

#### 254 **References:**

255

- 256 Halsall, C. J., Gevao, B., Howsam, M., Lee, R. G. M., Ockenden, W. A., & Jones, K. C. (1999). Temperature  
257 dependence of PCBs in the UK atmosphere. *Atmospheric Environment*, 33(4), 541-552. doi:  
258 10.1016/S1352-2310(98)00288-X
- 259 Hillery, B. R., Basu, I., Sweet, C. W., & Hites, R. A. (1997). Temporal and spatial trends in a long-term study of  
260 gas-phase PCB concentrations near the Great Lakes. *Environmental Science and Technology*, 31(6),  
261 1811-1816. doi: 10.1021/es960990h
- 262 Hoff, R. M., Mulr, D. C. G., & Grift, N. P. (1992). Annual cycle of polychlorinated biphenyls and organohalogen  
263 pesticides in air in Southern Ontario. 2. Atmospheric transport and sources. *Environmental Science and  
264 Technology*, 26(2), 276-283.
- 265 Hornbuckle, K. C., & Eisenreich, S. J. (1996). Dynamics of gaseous semivolatile organic compounds in a terrestrial  
266 ecosystem - effects of diurnal and seasonal climate variations. *Atmospheric Environment*, 30(23),  
267 3935-3945. doi: 10.1016/1352-2310(96)00135-5
- 268 Iwata, H., Tanabe, S., Sakai, N., & Tatsukawa, R. (1993). Distribution of persistent organochlorines in the oceanic  
269 air and surface seawater and the role of ocean on their global transport and fate. *Environ Sci Technol*, 27(6),  
270 1080-1098. doi: 10.1021/es00043a007
- 271 Jeeshim. (2003). Multicollinearity in Regression Models. from <http://php.indiana.edu/~kucc625>
- 272 Li, Q., Wang, X., Song, J., Sui, H., Huang, L., & Li, L. (2012). Seasonal and diurnal variation in concentrations of  
273 gaseous and particulate phase endosulfan. *Atmospheric Environment*, 61, 620-626. doi:  
274 10.1016/j.atmosenv.2012.07.068
- 275 Li, Q., Wang, X., Wang, R., Sui, H., Li, W., & Li, L. (2011). Seasonal trends and potential sources of ambient air  
276 OCPs in urban and suburban areas in Dalian, China. *Journal of Environmental Monitoring*, 13(6),  
277 1816-1822. doi: 10.1039/c0em00355g
- 278 Malaiyandi, M., & Shah, S. M. (1984). Evidence of photoisomerization of hexachlorocyclohexane isomers in the  
279 ecosphere. *Journal of Environmental Science and Health - Part A Environmental Science and Engineering*,  
280 19(8), 887-910.
- 281 Venier, M., & Hites, R. A. (2010). Regression model of partial pressures of PCBs, PAHs, and organochlorine  
282 pesticides in the Great Lakes' atmosphere. *Environmental Science and Technology*, 44(2), 618-623. doi:  
283 10.1021/es902804s
- 284 Willett, K. L., Ulrich, E. M., & Hites, R. A. (1998). Differential toxicity and environmental fates of  
285 hexachlorocyclohexane isomers. *Environmental Science and Technology*, 32(15), 2197-2207. doi:  
286 10.1021/es9708530

287

Table 1. Multiple regression (enter method) results for gaseous HCHs

		$\ln P=b_0+b_1 (1/T)+b_2 WS+b_3 \sin WD+b_4 \cos WD$						
		$\alpha$ -HCH			$\gamma$ -HCH			
		UC	SE	Sig.	UC	SE	Sig.	
Day (n=50)	b0	-19	4.2	1.0E-5	-15	3.6	1.2E-4	
	b1	-4,400	1,200	0.011	-5,800	1,000	1.4E-6	
	b2	0.13	0.06	0.042	0.083	0.062	0.14	
	b3	-0.42	0.21	0.051	0.083	0.18	0.65	
	b4	-0.40	0.21	0.052	0.064	0.18	0.76	
Night (n=49)	b0	-27	5.3	5.9E-6	-22	4.4	1.4E-5	
	b1	-1,800	1,500	0.23	-3,800	1,200	3.9E-3	
	b2	0.064	0.093	0.94	0.012	0.073	0.89	
	b3	-0.48	0.24	0.051	-0.25	0.19	0.22	
	b4	-0.043	0.25	0.87	-0.052	0.21	0.82	

$T$  is temperature in K;  $WS$  is wind speed in mph;  $WD$  is wind direction in degree. UC is unstandardized coefficient; SE is std. error.

$\alpha$ -HCH: Integrated correlation coefficient  $R^2=0.41$  and Sig. (F-test)=0.04 during daytime. Integrated correlation coefficient  $R^2=0.13$  and Sig. (F-test)=0.18 at night;

$\gamma$ -HCH: Integrated correlation coefficient  $R^2=0.45$  and Sig. (F-test)=2.38E-5 during daytime. Integrated correlation coefficient  $R^2=0.24$  and Sig. (F-test)=0.02 at night.

Table 2. Multiple regression (enter method) results for particle-associated HCHs

		$\ln P=b_0+b_1 (1/T)+b_2 WS+b_3 \sin WD+b_4 \cos WD$						
		$\alpha$ -HCH			$\gamma$ -HCH			
		UC	SE	Sig.	UC	SE	Sig.	
Day (n=45)	b0	-44	5.8	2.7E-9	-42	3.9	3.0E-13	
	b1	2,000	1,600	0.23	1,200	1,100	0.29	
	b2	-7.0E-3	0.093	0.94	-0.033	0.064	0.63	
	b3	0.11	0.29	0.71	-0.27	0.19	0.19	
	b4	-0.093	0.29	0.75	-0.19	0.20	0.35	
Night (n=43)	b0	-39	7.0	2.0E-6	-39	4.5	2.3E-10	
	b1	640	2,000	0.75	260	1,200	0.84	
	b2	-0.034	0.11	0.81	-0.082	0.072	0.25	
	b3	0.33	0.33	0.32	-0.39	0.21	0.071	
	b4	-0.27	0.36	0.46	-0.22	0.22	0.33	

$\alpha$ -HCH: Integrated correlation coefficient  $R^2=0.06$  and Sig. (F-test)=0.68 during daytime. Integrated correlation coefficient  $R^2=0.05$  and Sig. (F-test)=0.79 at night;

$\gamma$ -HCH: Integrated correlation coefficient  $R^2=0.08$  and Sig. (F-test)=0.51 during daytime. Integrated correlation coefficient  $R^2=0.16$  and Sig. (F-test)=0.17 at night.

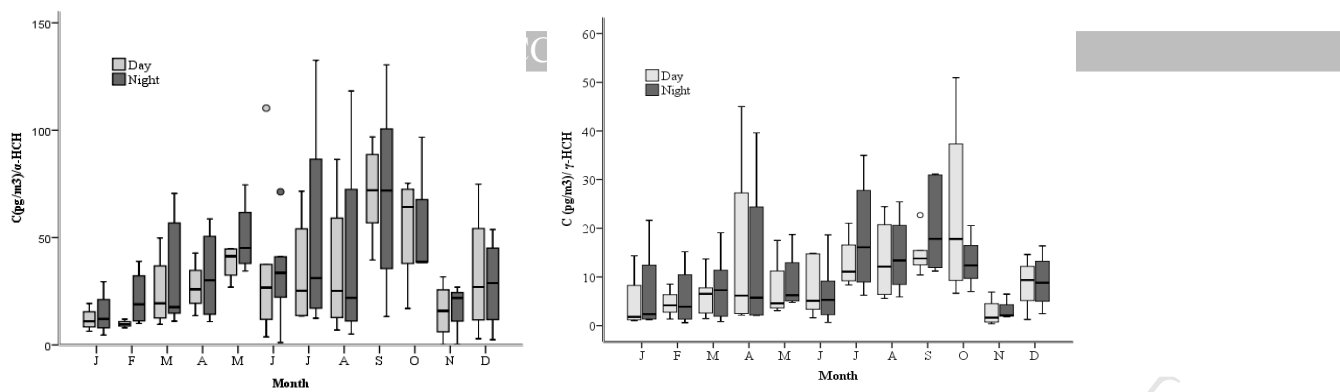


Figure 1. Monthly variations in  $\alpha$ -HCH (left panel) and  $\gamma$ -HCH (right panel) concentrations in gas phase

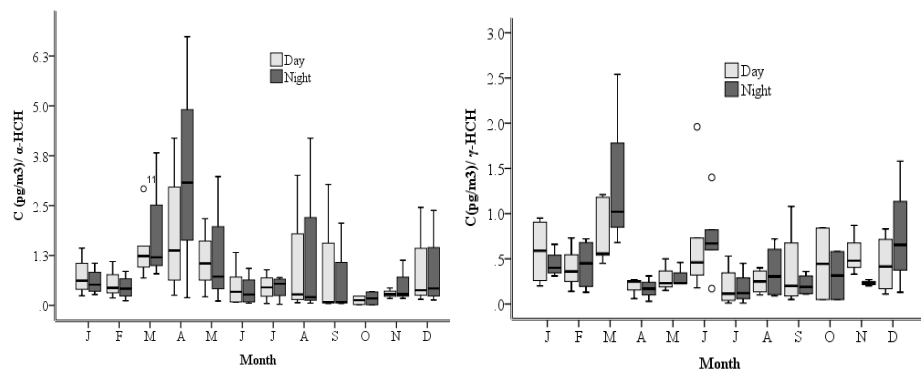


Figure 2. Monthly variations in  $\alpha$ -HCH (left panel) and  $\gamma$ -HCH (right panel) concentrations in particle-associated phase

ACCEPTED MANUSCRIPT

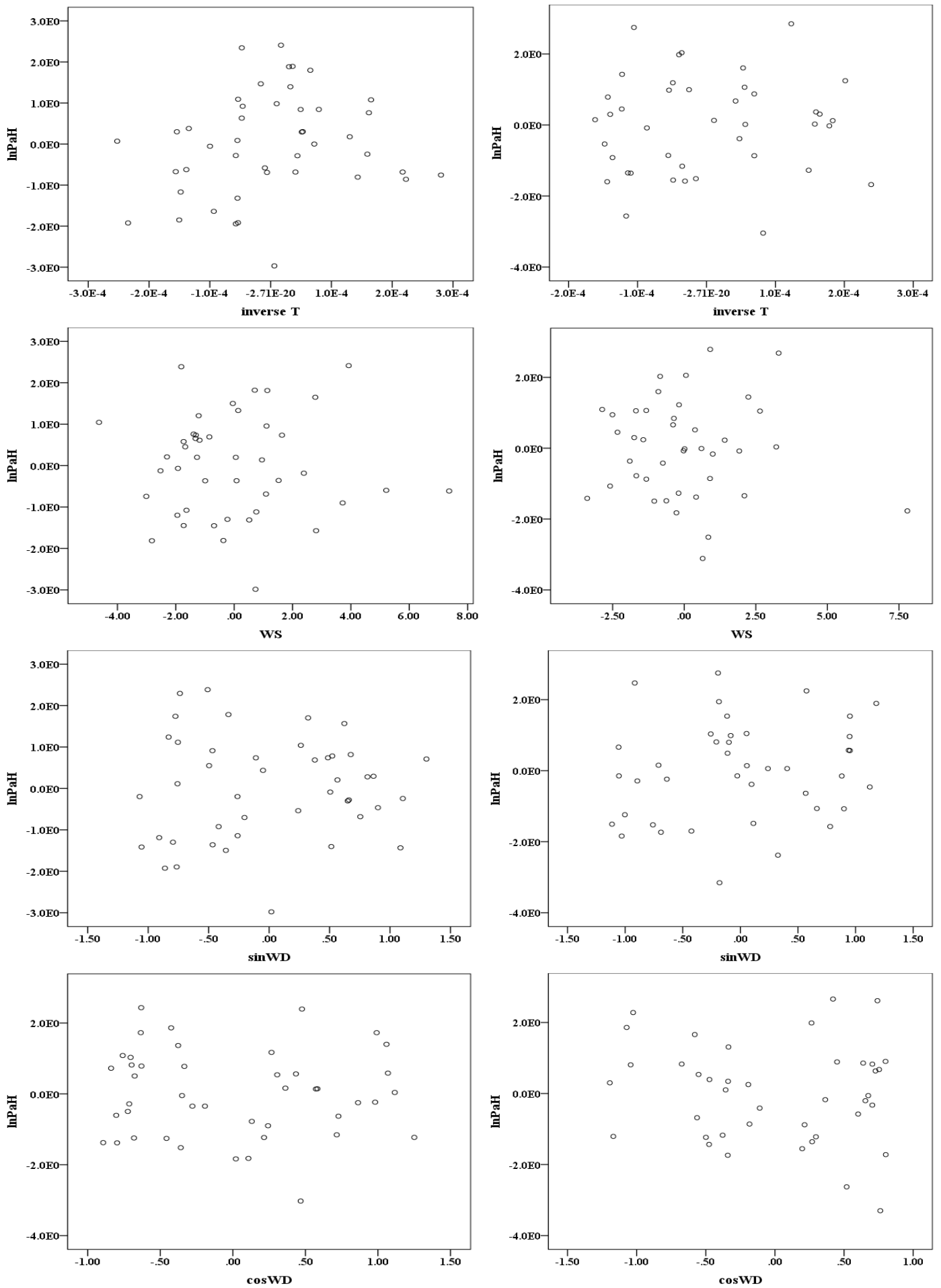


Figure 3. Partial regression of  $\alpha$ -HCH (day on the left and night on the right) in particle-associated phase against meteorological

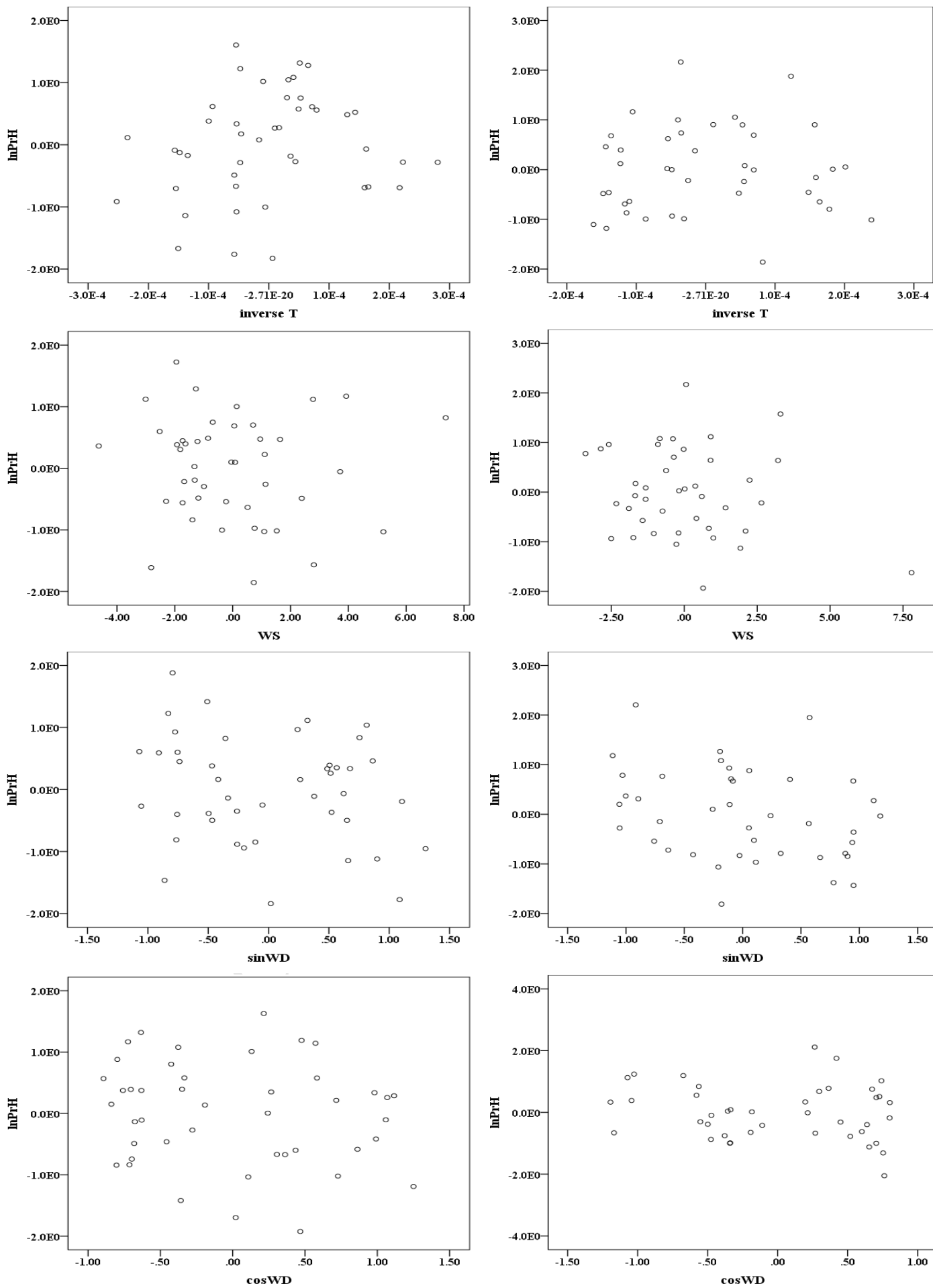


Figure 4. Partial regression of  $\gamma$ -HCH (day on the left and night on the right) in particle-associated phase against meteorological parameters

**Highlights**

- Diurnal and seasonal variations of HCHs in Dalian air are first time reported
- Gaseous and particle-associated HCHs peaked in autumn and spring respectively
- Multiple regression analysis was used to assess impact of meteorological parameters
- Concentration of particle-associated HCHs tended to remain stable



## Supplementary information

Analysis for Sources of Atmospheric  $\alpha$ - and  $\gamma$ -HCH in Gas and Particle-associated Phase in Dalian, China by Multiple Regression

QINGBO LI\*†, YAN LI††, XIANYU WANG††, RUIQI ZHANG†††, JIANMIN MA††††, MENGXUE SUN†, XIAONING LV†, JIAOLING BAO†

† College of Environmental Science and Engineering, Dalian Maritime University, Dalian 116026, China

††National Research Centre for Environmental Toxicology, The University of Queensland, 39 Kessels Road, Coopers Plains, QLD, 4108, Australia

†††Shaanxi University of Science & Technology, Shaanxi 710021, China

††††Key Laboratory of Western China's Environmental System, Ministry of Education, College of Earth and Environment Sciences, Lanzhou University, Lanzhou 730000, China

No. of pages: 7

Table S1. Atmospheric concentrations of gaseous  $\alpha$ - and  $\gamma$ -HCH ( $\text{pg m}^{-3}$ ) and  $C_{\alpha\text{-HCH}}/C_{\gamma\text{-HCH}}$  at the sampling site

		n	$\alpha$ -HCH				$\gamma$ -HCH				$C_{\alpha\text{-HCH}}/C_{\gamma\text{-HCH}}$			
			Mean	S.D	Min	Max	Mean	S.D	Min	Max	Mean	S.D	Min	Max
Spring (Mar-May)	Day	13	30	14	9.6	50	9.3	12	1.5	45	5.7	3.6	0.95	12
	Night	13	38	23	11	75	10	11	0.8	40	7.4	6.1	1.2	19
Summer (Jun-Aug)	Day	13	36	33	3.8	110	11	7.0	1.6	24	3.7	3.0	0.41	11
	Night	13	42	41	1.1	130	13	9.9	0.66	35	4.4	4.6	0.20	18
Autumn (Sep-Nov)	Day	13	49	31	0.071	97	14	13	0.37	51	5.3	3.5	0.19	11
	Night	11	52	42	0.36	130	14	10	1.8	31	4.3	4.2	NA	14
Winter (Dec-Feb)	Day	11	19	20	2.9	75	6.2	5.3	0.99	15	3.8	2.8	NA	8.3
	Night	12	22	16	2.5	54	7.3	7.0	0.60	22	6.9	11	0.66	42
Annual (Jan-Dec)	Day	50	34	27	0.074	110	10	10	0.37	51	4.7	3.3	NA	12
	Night	49	32	29	0.36	133	11	9.6	0.60	40	5.7	7.0	NA	42

**NB: Mean is arithmetic mean value; S.D is standard deviation; Min is minimum value; Max is maximum value; NA means that the value is not available**

Table S2. Atmospheric concentrations of particle-associated  $\alpha$ - and  $\gamma$ -HCH ( $\text{pg m}^{-3}$ ) and  $C_{\alpha\text{-HCH}}/C_{\gamma\text{-HCH}}$  at the sampling site

		n	$\alpha$ -HCH				$\gamma$ -HCH				$C_{\alpha\text{-HCH}}/C_{\gamma\text{-HCH}}$			
			Mean	S.D	Min	Max	Mean	S.D	Min	Max	Mean	S.D	Min	Max
Spring (Mar-May)	Day	12	3.0	2.3	0.43	8.4	0.51	0.35	0.15	1.2	16	3.6	2.0	19
	Night	9	3.3	2.8	0.22	7.6	1.1	0.89	0.23	2.5	3.4	3.1	0.96	12
Summer (Jun-Aug)	Day	13	0.81	0.75	0.091	2.7	0.42	0.50	0.071	2.0	14	2.8	0.091	9.8
	Night	13	1.3	2.2	0.054	8.4	0.51	0.39	0.10	1.4	3.8	4.6	0.12	13
Autumn (Sep-Nov)	Day	9	0.97	1.9	0.043	6.1	0.45	0.38	0.052	1.1	1.2	1.7	0.56	5.6
	Night	9	0.93	1.4	0.032	4.1	0.24	0.16	0.051	0.58	3.2	3.9	0.58	11
Winter (Dec-Feb)	Day	11	1.5	1.4	0.30	4.9	0.48	0.32	0.11	0.95	3.8	4.1	0.50	14
	Night	12	1.3	1.2	0.23	4.8	0.54	0.39	0.13	1.6	2.8	2.2	0.39	6.8
Annual (Jan-Dec)	Day	45	1.6	1.8	0.041	8.4	0.46	0.38	0.051	2.0	9.2	4.2	0.092	19
	Night	43	1.6	2.1	0.032	8.4	0.58	0.56	0.054	2.5	3.3	3.5	0.12	13

Table S3.  $C_{\text{gas}}/C_{\text{particle}}$  for  $\alpha$ - and  $\gamma$ -HCH at the sampling site

		n	$\alpha$ -HCH				$\gamma$ -HCH			
			Mean	S.D	Min	Max	Mean	S.D	Min	Max
Spring (Mar-May)	Day	12	21	25	3.2	84	30	47	2.7	180
	Night	9	46	64	2.9	160	38	41	2.8	130
Summer (Jun-Aug)	Day	13	120	200	NA	740	130	270	NA	1,000
	Night	13	140	150	2.1	420	220	560	2.8	2,100
Autumn (Sep-Nov)	Day	9	290	360	0.21	1,100	170	330	1.1	1,000
	Night	9	120	160	0.64	400	48	41	NA	100
Winter (Dec-Feb)	Day	11	31	69	NA	250	13	12	NA	42
	Night	12	36	54	3.7	200	17	19	0.83	58
Annual (Jan-Dec)	Day	45	100	210	NA	1,100	79	210	NA	1,000
	Night	43	85	120	0.64	420	88	310	NA	2,100

Table S4. Multicollinearity diagnostics of multiple regressions (enter method) (gas phase)

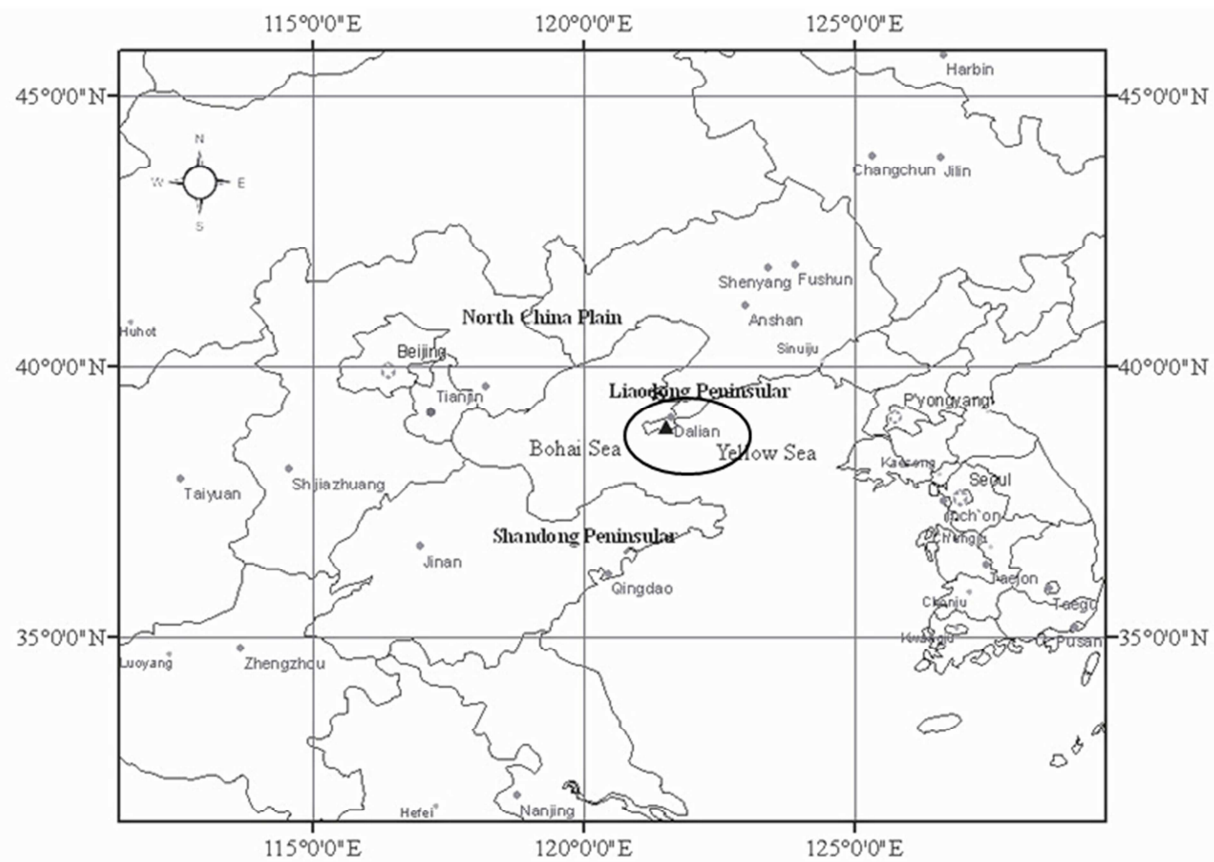
	Dimension	Eigenvalue	Condition index	Variance proportions				VIF	
				Inverse T	WS	sinWD	cosWD		
Daytime	$\alpha$ -HCH	1	2.982	1.000	0.00	0.02	0.00	0.01	
		2	1.103	1.644	0.00	0.00	0.53	0.29	1.064
		3	0.791	1.942	0.00	0.00	0.41	0.69	1.017
		4	0.123	4.924	0.00	0.98	0.01	0.00	1.086
		5	<b>0.001</b>	<b>73.379</b>	<b>1.00</b>	0.00	0.05	0.01	1.031
	$\gamma$ -HCH	1	2.982	1.000	0.00	0.02	0.00	0.01	
		2	1.103	1.644	0.00	0.00	0.53	0.29	1.064
		3	0.791	1.942	0.00	0.00	0.41	0.69	1.017
		4	0.123	4.924	0.00	0.98	0.01	0.00	1.086
		5	<b>0.001</b>	<b>73.379</b>	<b>1.00</b>	0.00	0.05	0.01	1.031
Nighttime	$\alpha$ -HCH	1	2.881	1.000	0.00	0.03	0.00	0.02	
		2	1.120	1.604	0.00	0.01	0.57	0.23	1.073
		3	0.760	1.948	0.00	0.00	0.38	0.74	1.060
		4	0.238	3.477	0.00	0.92	0.04	0.00	1.070
		5	<b>0.000</b>	<b>76.771</b>	<b>1.00</b>	0.04	0.01	0.02	1.053
	$\gamma$ -HCH	1	2.881	1.000	0.00	0.03	0.00	0.02	
		2	1.120	1.604	0.00	0.01	0.57	0.23	1.073
		3	0.760	1.948	0.00	0.00	0.38	0.74	1.060
		4	0.238	3.477	0.00	0.92	0.04	0.00	1.070
		5	<b>0.000</b>	<b>76.771</b>	<b>1.00</b>	0.04	0.01	0.02	1.053

Table S5. Multicollinearity diagnostics of multiple regressions (enter method) (particle-associated phase)

	Dimension	Eigenvalue	Condition index	Variance proportions				VIF	
				Inverse T	WS	sinWD	cosWD		
Daytime	$\alpha$ -HCH	1	2.958	1.000	0.00	0.02	0.00	0.01	
		2	1.075	1.659	0.00	0.00	0.55	0.28	1.104
		3	0.834	1.883	0.00	0.00	0.35	0.70	1.022
		4	0.132	4.732	0.00	0.97	0.02	0.00	1.121
		5	<b>0.001</b>	<b>72.238</b>	<b>1.00</b>	0.00	0.08	0.01	1.022
	$\gamma$ -HCH	1	2.958	1.000	0.00	0.02	0.00	0.01	
		2	1.075	1.659	0.00	0.00	0.55	0.28	1.104
		3	0.834	1.883	0.00	0.00	0.35	0.70	1.022
		4	0.132	4.732	0.00	0.97	0.02	0.00	1.121
		5	<b>0.001</b>	<b>72.238</b>	<b>1.00</b>	0.00	0.08	0.01	1.022
Nighttime	$\alpha$ -HCH	1	2.906	1.000	0.00	0.03	0.00	0.02	
		2	1.151	1.589	0.00	0.01	0.51	0.21	1.050
		3	0.682	2.064	0.00	0.00	0.44	0.76	1.057
		4	0.260	3.342	0.00	0.91	0.04	0.00	1.096
		5	<b>0.001</b>	<b>74.645</b>	<b>1.00</b>	0.04	0.01	0.00	1.070
	$\gamma$ -HCH	1	2.906	1.000	0.00	0.03	0.00	0.02	
		2	1.151	1.589	0.00	0.01	0.51	0.21	1.050
		3	0.682	2.064	0.00	0.00	0.44	0.76	1.057
		4	0.260	3.342	0.00	0.91	0.04	0.00	1.096
		5	<b>0.001</b>	<b>74.645</b>	<b>1.00</b>	0.04	0.01	0.00	1.070

Table S6. Parameters of regression model running under stepwise method for gaseous HCHs

	Model (Stepwise)		Dimension	UC		SC	t	Sig.	Eigenvalue	Condition Index	Variance Proportions		VIF
	R <sup>2</sup>	p		B	Std.	Beta					1	2	
lnP $\alpha$ -HCH (Day)	0.2384	3.760E-4	(Constant)	-16.816	4.468	-.488	-3.763	4.648E-4	1.999	1.000	2.957E-4	2.957E-4	1.000
			inverseT	-4897.983	1278.109		-3.832	3.760E-4		.001	58.143	1.00	
lnP $\gamma$ -HCH (Day)	0.417	5.524E-7	(Constant)	-14.986	3.486	-.645	-4.299	8.576E-5	1.999	1.000	2.957E-4	2.957E-4	1.000
			inverseT	-5776.657	997.129		-5.793	5.524E-7		.001	58.143	1.00	
lnP $\alpha$ -HCH (Night)	0.324	0.026	(Constant)	-33.804	.162	-.324	-208.411	8.106E-69	1.018	1.000	.49	.49	1.000
			sinWD	-.520	.226		-2.297	.026		.982	1.018	.51	
lnP $\gamma$ -HCH (Night)	0.202	0.002	(Constant)	-21.001	4.165	-.449	-5.043	7.978E-6	1.999	1.000	2.650E-4	2.650E-4	1.000
			inverseT	-3974.350	1178.531		-3.372	.002		.001	61.414	1.00	



▲ Sampling site

Figure S1. Map of sampling site